Available online at www.sciencedirect.com
SCIENCE DIRECT®
Surface Science 575 (2005) 60–68
SURFACE SCIENCE
www.elsevier.com/locate/susc

The nucleation sites of Ag clusters grown by vapor deposition on a $TiO_2(1\,1\,0)$-1×1 surface

Xiao Tong *, Lauren Benz, Andrei Kolmakov, Steeve Chrétien, Horia Metiu, Steven K. Buratto *

Department of Chemistry and Biochemistry, University of California, Santa Barbara, CA 93106-9510, USA

Received 14 June 2004; accepted for publication 2 November 2004
Available online 19 November 2004

Abstract

We present results of a scanning tunneling microscopy (STM) study of the nucleation and growth of silver clusters grown by vapor deposition on a rutile $TiO_2(1\,1\,0)$-1×1 surface. We have scanned, with atomic resolution, the same surface area before and after Ag deposition, to determine the relationship between the nucleation sites and various surface defects. We have found that small precursor strands of (1×2) surface reconstruction have a higher propensity to nucleate Ag clusters than missing-oxygen vacancies and C-type defects. All studies were performed at room temperature, a regime in which the clusters nucleate and grow during the deposition, but do not coarsen.

Keywords: Defects; Clusters; Nucleation; Scanning tunneling microscopy; Silver; Titanium oxide

1. Introduction

Metal nanoclusters supported on a TiO_2 surface are used as catalysts [1–5] and chemical sensors [6]. In most surface science work on these systems the clusters are prepared by vapor deposition. Despite the large number of interesting studies [7–12], the mechanism of cluster nucleation, growth and sintering is not fully understood. These processes are complicated by the existence, on the oxide surface, of missing-oxygen vacancies, hydroxyls, steps, patches of reconstructed surface and features of unknown origin that often are visible in STM. The fact that the type and abundance of imperfections of the surface depends on the method of preparation creates additional scatter in STM data.

This situation has prompted us to examine the connection between the location of clusters prepared by vapor deposition, and the location of various surface defects prior to deposition. To do this we have scanned, with atomic resolution, the

* Corresponding authors. Tel.: +1 805 893 3393; fax: +1 805 893 4120 (S.K. Buratto). Tel.: +1 805 893 3700 (X. Tong).
E-mail addresses: xtong@chem.ucsb.edu (X. Tong), buratto@chem.ucsb.edu (S.K. Buratto).

0039-6028/$ - see front matter © 2004 Elsevier B.V. All rights reserved.
doi:10.1016/j.susc.2004.11.003

same area before and after deposition. This allows us to establish semi-quantitatively which defects are more effective nucleation centers.

2. Experimental

All experiments were performed in an ultrahigh vacuum (UHV) chamber with a base pressure of less than 2×10^{-10} Torr, equipped with an RHK-300 variable temperature STM. The clean $TiO_2(1\,1\,0)$-1×1 surface was prepared with multiple cycles of Ar-ion sputtering (1 keV, 20 min) of the crystal (Commercial Crystal Laboratories), followed by annealing at 1000 K for 20 min. This procedure produced a surface with an average terrace width of 25 nm. Auger spectra of the surface were taken before and after deposition.

Ag was deposited from a collimated, homemade Ag vapor source in which a current was passed through a tungsten wire basket containing high-purity Ag pellets (99.999%). All depositions were performed at room temperature. The metal deposition was performed directly on the tunneling junction, under a grazing angle of approximately 60° with respect to the normal [13]. This method was chosen to facilitate scanning the same area both before and after deposition. The average flux was calculated to be 0.03 ML/min (a monolayer corresponds to 1.39×10^{15} atoms/cm^2, the surface concentration of Ag(1 1 1)), and the exposure was controlled with a beam shutter.

The STM data were obtained in constant current mode, at sample biases of +1 to +2 V, and tunneling currents between 0.1 and 0.2 nA; the electrons tunneled into the empty states of the surface. The STM tips were made from electrochemically etched tungsten wire and were subsequently cleaned in UHV by electron bombardment. The measured cluster diameters were not corrected for the size and shape of the tip, and are used for qualitative characterization only.

3. Results

We show in Fig. 1 an image of the clean surface with various kinds of defects prior to Ag deposition. Previous STM studies have already identified some of the features seen in this figure: the bright rows are the 5-fold coordinated Ti atoms (5c-Ti) and the dark troughs are the bridging-oxygen rows [7]. For describing the other features seen in Fig. 1, we use the nomenclature introduced by Diebold et al. [14]. The type A-defects are located on the bridging-oxygen rows and are either bridging-oxygen vacancies or hydroxyls formed at the bridging-oxygen atoms. We were able to distinguish the vacancies from the bridging hydroxyl groups by careful tuning of the imaging conditions [14–16]. The brighter white spots between the Ti rows (circled with a solid line in Fig. 1a) are bridging-oxygen vacancies; the dimmer white spots, also

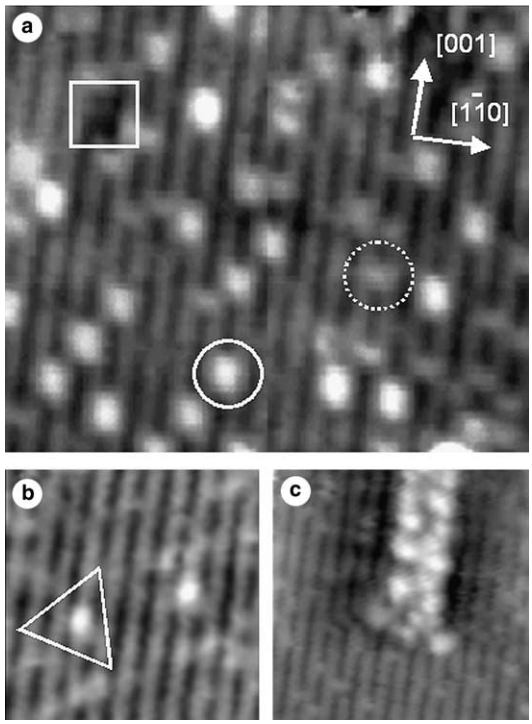

Fig. 1. (a) An STM image (110 Å × 110 Å) of a clean $TiO_2(1\,1\,0)$ surface. The bright protrusion between the Ti rows indicated by a solid circle is an oxygen vacancy; the slightly dimmer protrusion between the Ti rows, indicated by a dashed circle, is a hydroxyl group (both are called type A defects); the dark feature on the Ti row, indicated by a square, is of unknown origin (type B defect). (b) A bright feature located on a Ti row indicated by a triangle, is of unknown origin (type C-defect). (c) A strand of 1×2 precursors.

located between the 5c-Ti rows, (circled with a hatched line in Fig. 1a), are bridging hydroxyl groups. In agreement with a previous study [17], the main differences between these features are their extents in the [0 0 1] direction (8.9 Å for a vacancy and 6.9 Å for a hydroxyl group) and their apparent heights (0.4 Å for a vacancy and 0.3 Å for a hydroxyl group, also measured along [0 0 1]).

The surfaces we have studied show the presence of type-A defects at a level of 12% relative to the number bridging O atoms present on a stoichiometric surface. Among these types of defects, 60% are oxygen vacancies. It is likely that the hydroxyl groups are responsible for the remaining 40% of the type A defects due to the dissociation of residual water molecules on the surface. Neither the vacancies nor the hydroxyl groups are mobile at room temperature in UHV, as we have observed no migration after scanning the surface for 1 h. The dark features located on the 5c-Ti rows (marked with a square in Fig. 1a), which can occupy from one to several surface unit cells, are called type B-defects [14]. The coverage of these defects is 0.3% on our sample. These features were tentatively assigned as subsurface oxygen vacancies, however, first-principle total-energy calculations show that such a configuration is highly unlikely [14], therefore their chemical identity remains unknown. The bright protrusions which appear on the 5-coordinate Ti rows (marked with a triangle in Fig. 1b) are called type C-defects [14]. The concentration of these defects is below the sensitivity of our Auger and XPS instruments, so their chemical nature is unknown. Recently it was shown that charged subsurface impurities in titania can locally modulate the band bending and therefore may influence surface adsorption and/or nucleation phenomena [18]. We have not detected such features in this study.

Fig. 1c and Fig. 2a display two types of extended line defects, which often appear on the reduced $TiO_2(1\,1\,0)$ surface, and affect nucleation. These are precursors for (1×2) reconstruction, and step edges [19]. The (1×2) precursors are seen as bright patches, and most often occur on the down side of a step. The one shown in Fig. 1c has an elongated shape and is oriented parallel to the bridging-oxygen rows. The measured corrugation of the (1×2) strands is ~1.8 A, and according to Onishi's model [20,21], the stoichiometry of these types of strands is Ti_2O_3. The morphology of the step edges seen in Fig. 2a is typical of a moderately reduced $TiO_2(1\,1\,0)$ surface.

Fig. 2a shows a clean TiO_2 surface with a high density of point and line defects; Fig. 2b displays the *same area* after we have deposited approximately 0.06 ML of Ag in 2 min. The deposited atoms have enough mobility on the surface at room temperature to form clusters with diameters of 3.6–4.8 nm, and a heights of 0.7–0.9 nm, roughly corresponding to two or three atomic Ag layers. We have scanned some of the samples for as long as an hour, and observed no change in the number of clusters, their size or shape; therefore we observe island nucleation and growth (during deposition), free of coarsening. By comparing the two figures we can determine the sites where nucleation takes place, as circled in 2a.

The images in Fig. 2c–f are enlargements of sections taken from Fig. 2a which show a few areas where nucleation occurred. Fig. 2c shows an area that has several missing-oxygen vacancies; 2d shows a site near a step edge; 2e shows a site where nucleation occurred close to a 1×2 precursor; and 2f shows a nucleation site near a type C-defect. We remind the reader that the circles in Fig. 2c–f overestimate the diameter of the cluster, since we have not corrected the images for tip-size effects. Additional detailed and important observations can be made from a qualitative analysis of Fig. 2 and additional images.

Regarding the nucleation of clusters by oxygen vacancies, Fig. 2c shows an area on the clean surface that is covered by a cluster after deposition. This area contains oxygen vacancies only. Therefore, we assume that nucleation at this site is a result of the presence of bridging-oxygen vacancies, without interference from neighboring defects. By examining many images, we have found that the center of the clusters is located in the vicinity of, but not centrally on a missing-oxygen vacancy. In separate experiments we use the tip to move the clusters (with rapid scanning and without deteriorating the tip condition) from their original positions, and inspect the area underneath. Fig. 3a shows three Ag clusters on a $TiO_2(1\,1\,0)$-1×1

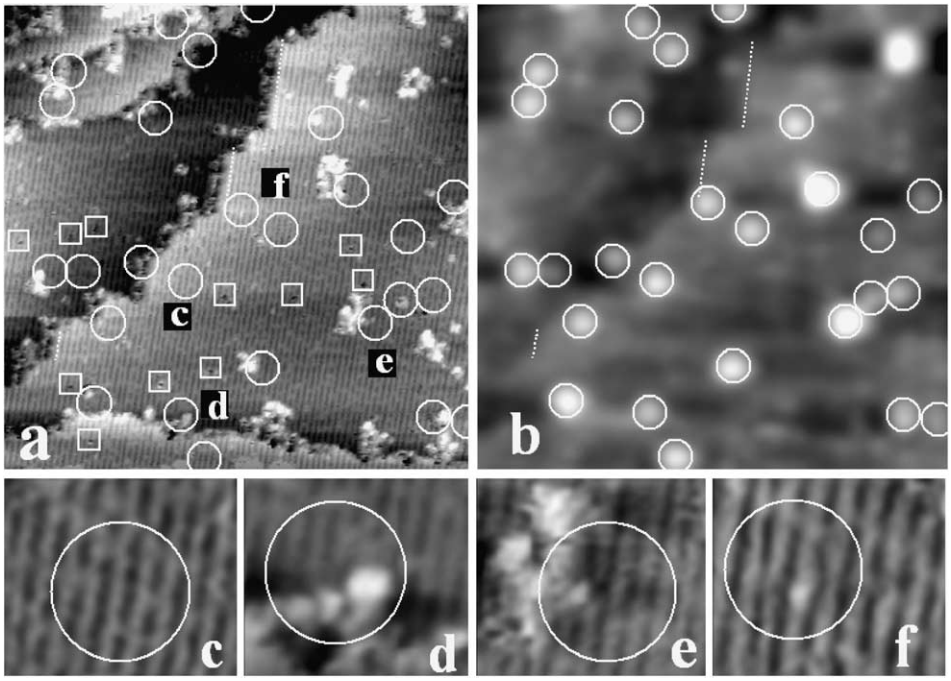

Fig. 2. STM images show (a) a clean $TiO_2(1\,1\,0)$-1×1 surface (500 Å × 500 Å). (b) The same area after exposure to 0.06 ML of Ag. The white circles in (a) indicate the nucleation positions of the Ag clusters determined by comparison with (b). The tunneling conditions in (b) were adjusted to avoid tip–cluster interaction. Images (c)–(f) are enlarged areas of (a) which show the preferential nucleation sites of Ag clusters around oxygen vacancies, step edges, 1×2 strands and type C-defects, respectively. No clusters are found at type B-dark defects (marked with squares in (a)).

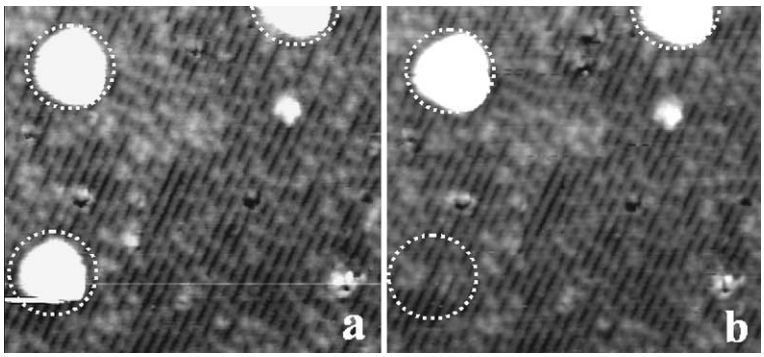

Fig. 3. (a) An STM image (200 Å × 180 Å) shows three Ag clusters distributed on a clean $TiO_2(1\,1\,0)$ surface with oxygen vacancies. (b) One of the three clusters in (a) was removed using the STM tip. The area underneath the removed cluster as indicated by the circle shows a similar density of oxygen vacancies as the clean area. There are neither clusters nucleated at dark defects on Ti rows, nor dark defects underneath the removed cluster, implying that the dark defects on Ti rows are not preferential nucleation sites for Ag clusters.

surface that has a high density of A-type defects, which are seen as faint white spots. Fig. 3b shows the same area, after one cluster was removed with the STM tip, demonstrating that the missing-oxygen vacancies are not located directly beneath the center of the cluster.

In the case of the dark defects, we see in Fig. 2 that no clusters are found at type B-dark defects

on Ti rows (marked with a square in Fig. 2a). Fig. 3 also reveals that there are neither clusters nucleated at dark defects on Ti rows, nor dark defects underneath the removed cluster. These observations imply that the dark defects on the Ti rows are not preferential nucleation sites for Ag clusters.

We have found, on surfaces prepared from the same sample, by the same method, quite a bit of variation regarding nucleation at steps. In some images (such as in Fig. 2a) the steps have a large number of patches of incipient 1×2 reconstruction. When this is the case almost all clusters formed near the step are located next to these patches. The density of clusters near such steps is small, as compared to the density on the terrace. The situation is different in the scans shown in Fig. 4a, which show that clusters are formed on both the steps and the terraces, and that the cluster density on a terrace is higher, the broader the terrace. In Fig. 4c, we show the clusters formed by depositing more Ag on the surface shown in Fig. 4a. We see that this results in a considerable increase of about a factor of 2 in the density of clusters on the terrace, without an increase of the density at the steps. The result of further deposition, on the area imaged in Fig. 4c, is shown in Fig. 4d. It is interesting to see that Ag does not form extended islands or a continuous film, but prefers to form distinct clusters. This is an indication of a very small diffusion length and also of the tendency of Ag not to wet the TiO_2 surface.

In Fig. 4e and f, which were enlarged from the areas marked with white squares in Fig. 4b, we show a few steps and also indicate the direction of the bridging-oxygen rows. The steps make an angle with the rows, and in doing so they consist of short steps nearly perpendicular to the rows ($[1\,\bar{1}\,1]$ direction) and short steps parallel to them ([0 0 1] direction). The clusters are trapped by the short steps which run nearly perpendicular to the rows, however, they rarely nucleate on the steps running parallel to the bridging-oxygen rows, statistically. This suggests, but does not prove, that the Ag atoms travel more rapidly in the direction parallel to the bridging-oxygen rows. This will increase the flux of atoms to the steps nearly perpendicular to the bridging-oxygen rows. The fact that the step has a "saw tooth" shape on a short length scale is the reason that all steps have roughly the same cluster density, regardless of their orientation on a larger scale as indicated in Fig. 4a. In addition, Fig. 4f shows that clusters also appear to nucleate at kink positions where two steps meet. To summarize, there is a great variety of steps on the TiO_2 surface, and their ability to nucleate Ag clusters depends on their orientation, the presence of incipient 1×2 domains, and the size of the adjacent terraces.

The effect of 1×2 precursor strands on cluster nucleation has been examined in this study, and is found to be quite critical. Fig. 2e shows a site where nucleation occurs close to a 1×2 precursor. Fig. 5a shows an image of a surface that has several small 1×1 domains, while the rest of the 1×1 surface is covered with a high density of 1×2 precursor strands. Fig. 5b shows the same area after Ag deposition. Compared with the regular 1×1 domain, the cluster density is 7 times higher on the areas covered with strands of 1×2 precursors, which act as Ag atom traps and cause a lowering of the effective diffusion coefficient in these areas. A similar behavior was observed recently for Pd and Cu deposited on (1×1) and (1×2) TiO_2(1 1 0) surfaces [22,23].

Thus far we have presented the various types of defects present on the surface, and have given our observations regarding cluster nucleation at different sites. Careful statistical analysis of multiple images of the same area, taken before and after deposition, allows us to examine more quantitatively the propensity of various surface sites to nucleate Ag clusters. We give in Table 1 the surface density of various defect sites and the efficiency with which they nucleate clusters. To define the density of the sites at the border of the 1×2 strands we count the number of oxygen atoms along such borders, per unit area of the scanned surface. All other defect densities are defined as simply the number of defects per unit area. The ability of a defect of a given type to nucleate a cluster is characterized by the number of clusters at that type of site, divided by the number of such sites (column 4 in Table 1). Judged by this criterion the 1×2 edge sites are a factor of two more efficient than the C-sites, and nearly a factor of four

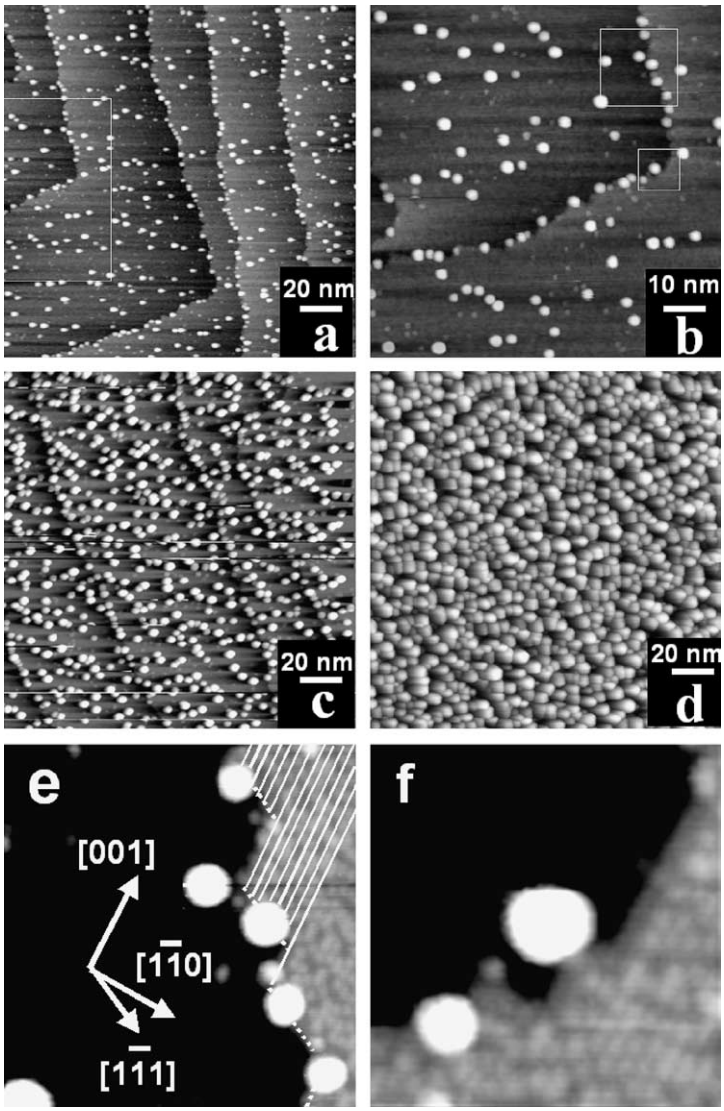

Fig. 4. (a) Ag clusters formed as a result of a low coverage deposition. The steps make an angle with the bridging-oxygen rows. (b) Image enlarged from area marked with square in (a). (c) The surface after further deposition of Ag on the area shown in (a). Notice a considerable increase in the number of clusters on the terrace versus the number on steps. (d) The same area after further deposition of Ag. It appears that Ag does not "wet" the TiO_2 surface as it does not produce a smooth film. Images (e) and (f) are enlarged from areas marked with squares in image (b). Bridging-oxygen rows indicated by the lines on the right-hand side of the figure, run along the [0 0 1] direction. The clusters are formed on the short step segments that are along the $[1\,\bar{1}\,1]$ direction. Clusters also appear to nucleate at kink positions where two steps meet as shown in (f).

more efficient than the missing-oxygen vacancies. The B-type "dark" features do not capture Ag atoms effectively. Given the great variety of behavior observed for nucleation at steps, we did not include the steps in Table 1.

4. Discussion

In addition to the different capturing abilities of various defects on the titania surface, several additional points can be addressed regarding the

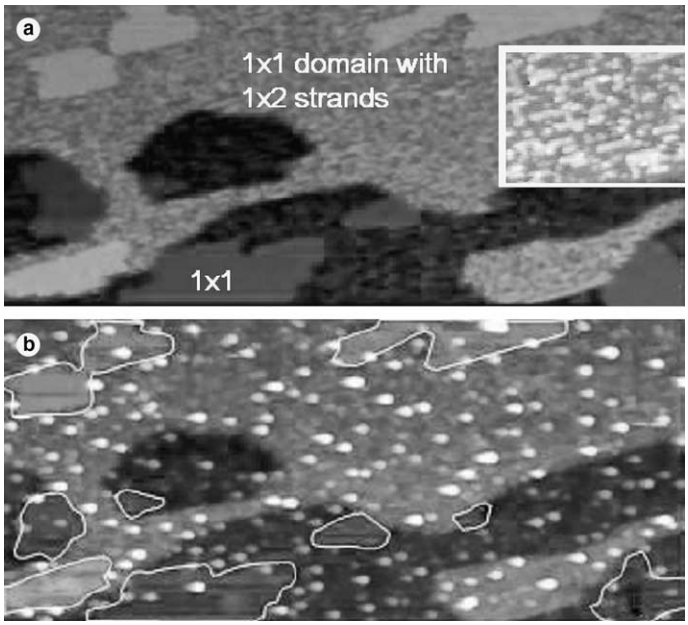

Fig. 5. (a) Several clean $TiO_2(1\,1\,0)$-1×1 domains surrounded by 1×1 domains with a high density of 1×2 strands (2000 Å × 850 Å). The darker the color, the lower the terrace imaged. The inset is an enlarged image of a 1×1 domain with strands on it. (b) The same area after Ag deposition. The Ag clusters preferentially nucleate on the regions with 1×2 strands; the presence of the strands lowers the effective diffusion coefficient of the Ag atoms.

Table 1
Raw data used to calculate the relative tendency of clusters to nucleate at various surface defect sites

Defect type	Defect density (# of defects/cm^2)	Density of clusters at defects (# of clusters at defect site/cm^2)	Nucleation tendency
Oxygen vacancies	3.6×10^{13}	2.6×10^{11}	7.2×10^{-3}
1×2 Edge sites	1.9×10^{13}	5.6×10^{11}	3.0×10^{-2}
C-type	1.4×10^{12}	2.0×10^{10}	1.4×10^{-2}
B-type	4.4×10^{11}	1.6×10^{8}	3.6×10^{-4}

Defect density is defined here as the number of defects per square centimeter. In the case of the 1×2 edge sites, we define the number of defects at such sites to be equivalent to the number of oxygen atoms along the borders of the 1×2 precursor regions. The density of clusters at each defect type (third column) is the number of clusters per unit area that nucleate at a particular defect. The ratio of the density of clusters at defects to the defect density gives what we define here as the nucleation tendency, which can be used to compare cluster nucleation at one site with another. The nucleation is highest for 1×2 precursors, followed by type C defects, and oxygen vacancies. Type B defects show practically no nucleation ability.

nucleation of Ag at defect sites. First, our STM images reveal that the centers of the clusters that are formed on top of an oxygen vacancy do not coincide with the vacancy site. If one assumes that the nucleation site must be at the center of the grown cluster, one would conclude that nucleation takes place *near* a missing-oxygen vacancy. We argue below that this is not the only interpretation compatible with our observations.

We have performed DFT calculations [24] which show that on a surface with no steps, the bond of an Ag atom to a missing-oxygen vacancy site is stronger by about 0.5 eV than the bond to any other site on a terrace (i.e. away from a step). Therefore, most Ag atoms landing initially on the surface travel on the terrace and are trapped either in an oxygen vacancy, or at a step (which also binds Ag strongly). Subsequent Ag atoms falling

on the surface have a more complicated fate. They can bind to the existing Ag atoms, contributing to cluster growth, or they can bind to an oxygen vacancy or a step, creating new nuclei. In addition, the binding energy of an Ag dimer at an oxygen vacancy site is comparable to the binding energy of the dimer to the stoichiometric (no vacancies, no defects, no steps) surface. Therefore, a dimer formed at an oxygen-vacancy site may leave it. Since its mobility is low, it is likely that the dimer will capture another silver atom before wandering too far from the oxygen vacancy. The mobility of the trimer formed in this way is likely to be very low. In time, the trimer will capture newly deposited Ag atoms and grow into a large Ag cluster that may extend to cover the vacancy. This vacancy will not be located at the center of the cluster it had nucleated.

Furthermore, since the clusters we observe are small, their growth around the point of formation is subject to large shape fluctuations, due to the stochastic nature of atom arrival at the border of the cluster and of the motion of the atoms around this border. Because of this, the nucleation sites of clusters grown under identical conditions are randomly located with respect to the center of the cluster.

Finally, one should keep in mind that nucleation is a kinetic phenomenon and the nuclei are not necessarily formed on the site where they have a minimum energy. If the dimer mobility is low, the nucleation takes place where two atoms (''walking'' at random on the surface) happen to meet, and this may be near an oxygen vacancy and not on it. Subsequent growth may extend the cluster over the vacancy, which results in the presence of a vacancy near the periphery of the cluster and not at its center. Nucleation did not take place at the oxygen vacancy that ends up accidentally under the cluster.

For the reasons described above, we do not wish to assume that the center of the cluster is the place where nucleation took place, nor do we assume that nucleation takes place near an oxygen vacancy. We note, however, that in a careful and interesting paper, Frenken's group [22] interpreted their data to mean that Pd clusters grown on $TiO_2(1\,1\,0)$ nucleate *near* missing-oxygen vacancies.

It has been previously reported that Au clusters on the $TiO_2(1\,1\,0)$-1×1 surface nucleate primarily at oxygen-vacancy sites. Furthermore, the deposition of metal leads to an accumulation of vacancies under the clusters, with a simultaneous reduction in the density of vacancies in the space between the clusters [11]. We do not observe this behavior for the Ag clusters. As shown in Fig. 3, after removing a cluster from its location, no accumulation of vacancies under the cluster is observed, and we see no decrease of vacancy density in the space between the clusters at room temperature. To understand why the behavior of Ag differs from that of Au we have calculated the binding energy of the Au and Ag monomers, dimers and trimers, to a vacancy site. We found that the binding energy of an Au atom to an oxygen-vacancy is about 1.5 times that of Ag. Since this binding energy is the ''thermodynamic force'' driving the accumulation of vacancies under the cluster, the difference in the binding energy may explain the difference between the behavior of Au and Ag.

The interplay between the mobility of the atoms, the deposition flux and the terrace width determines the density and the distribution of clusters formed by vapor deposition on the surface. Consider first the case when the surface has steps but it does not have any oxygen vacancies on the terraces between the steps. If the mobility of the Ag atoms on a terrace is high and the deposition flux is low, most of the deposited atoms reach the steps and stick to them. At any given time, the density of the atoms on the terrace is low and the chance that they meet accidentally on the terrace and form a nucleus is minimal. In such a case, most clusters will be located at the steps. This is not what we see in Fig. 4a and b, which show that the density of the clusters on the terrace is high. This happens because the missing-oxygen and the C-type defects trap the Ag atoms and only those that manage to avoid these traps reach a step.

We derive interesting information by comparing Fig. 4a with Fig. 4c. We show, in Fig. 4c, a surface produced by depositing additional Ag atoms on the surface imaged in Fig. 4a. The atoms landing on the surface imaged in Fig. 4a have three options: They can travel on the surface to meet an existing cluster and stick to it, or they can form a new

nucleus on the terrace, by sticking to an oxygen vacancy or a C-type defect. The increase of cluster density in Fig. 4c (as compared to Fig. 4a) indicates that the last possibility takes place rather frequently. However, not all deposited atoms have this fate. Some manage to reach the clusters present on the surface prior to the second deposition and cause them to grow. This is why the height of the clusters in Fig. 4c is about 30% higher that that in Fig. 4a. It is interesting to note that, in going from Fig. 4a to c, the density of clusters along the step does not increase. This is likely due to the fact that the saturation density of clusters is reached on the steps while it is not on terraces.

5. Summary

The same area of a titania sample has been imaged by STM both before and after Ag deposition with atomic resolution, allowing the determination of the propensity for nucleation at various defect sites. We observed that 1×2 surface strands, missing-oxygen vacancies, and C-type defects are preferential nucleation sites for Ag clusters, while dark defects are not. In particular, 1×2 surface strands are most effective in generating nuclei for cluster growth. We have found that the formation of an Ag cluster does not lead to an accumulation of oxygen vacancies under the cluster, as it does when Au is deposited. This difference between Ag and Au is made plausible by DFT calculations that show that the bonding of Ag, Ag_2 and Ag_3 to an oxygen vacancy is substantially weaker than that of the corresponding Au clusters. The same experiments at a range of temperatures and deposition fluxes will be conducted to make this study more quantitative.

Acknowledgments

We are particularly indebted to Paul Kemper, Yigal Lilach, and Manuel Manard for assistance with instrumentation. This work was funded by a Defense University of Research in Nanotechnology (DURINT) grant from the Airforce Office of Scientific Research (AFOSR).

References

[1] R.J. Lad, Surface Review and Letters 2 (1995) 109.
[2] D.W. Goodman, Surface Review and Letters 2 (1995) 9.
[3] U. Diebold, J.M. Pan, T.E. Madey, Surface Science 333 (1995) 845.
[4] C.T. Campbell, Surface Science Reports 27 (1997) 1.
[5] M. Baumer, H.J. Freund, Progress in Surface Science 61 (1999) 127.
[6] W. Gopel, Sensors and Actuators 16 (1989) 167.
[7] U. Diebold, Surface Science Reports 48 (2003) 53.
[8] H.J. Freund, Surface Science 500 (2002) 271.
[9] A. Sanchez, S. Abbet, U. Heiz et al., Journal of Physical Chemistry A 103 (1999) 9573.
[10] A.K. Santra, D.W. Goodman, Journal of Physics-Condensed Matter 15 (2003) R31.
[11] E. Wahlstrom, N. Lopez, R. Schaub et al., Physical Review Letters 90 (2003) 026101.
[12] A. Kolmakov, D.W. Goodman, Chemical Record 2 (2002) 446.
[13] A. Kolmakov, D.W. Goodman, Review of Scientific Instruments 74 (2003) 2444.
[14] U. Diebold, J. Lehman, T. Mahmoud et al., Surface Science 411 (1998) 137.
[15] S. Suzuki, K. Fukui, H. Onishi et al., Physical Review Letters 84 (2000) 2156.
[16] R. Schaub, E. Wahlstrom, A. Ronnau et al., Science 299 (2003) 377.
[17] R. Schaub, R. Thostrup, N. Lopez et al., Physical Review Letters 87 (2001) 3590.
[18] M. Batzill, E.L.D. Hebenstreit, W. Hebenstreit et al., Chemical Physics Letters 367 (2003) 319.
[19] R.A. Bennett, M.A. Newton, R.D. Smith et al., Materials Science and Technology 18 (2002) 710.
[20] H. Onishi, Y. Iwasawa, Surface Science 313 (1994) L783.
[21] H. Onishi, K. Fukui, Y. Iwasawa, Bulletin of the Chemical Society of Japan 68 (1995) 2447.
[22] M.J.J. Jak, C. Konstapel, A. van Kreuningen et al., Surface Science 474 (2001) 28.
[23] J. Zhou, D.A. Chen, Surface Science 527 (2003) 183.
[24] S. Chrétien, H. Metiu, to be published.